

A Rotation and a Translation Suffice: Fooling CNNs with Simple Transformations

Logan Engstrom *
MIT
engstrom@mit.edu

Dimitris Tsipras *
MIT
tsipras@mit.edu

Ludwig Schmidt
MIT
ludwigs@mit.edu

Aleksander Mądry
MIT
madry@mit.edu

Abstract

Recent work has shown that neural network-based vision classifiers exhibit a significant vulnerability to misclassifications caused by imperceptible but adversarial perturbations of their inputs. These perturbations, however, are purely pixel-wise and built out of loss function gradients of either the attacked model or its surrogate. As a result, they tend to be contrived and look pretty artificial. This might suggest that vulnerability to misclassification of slight input perturbations can only arise in a truly adversarial setting and thus is unlikely to be a problem in more benign “natural” contexts.

In this paper, we provide evidence that such belief might be incorrect. We demonstrate that significantly simpler, and more likely to occur naturally, transformations of the input – specifically, rotations and translations *alone*, suffice to significantly degrade the classification performance of neural network-based vision models across a spectrum of datasets. This remains to be the case even when these models are trained using appropriate data augmentation. Also, finding such “fooling” transformations does not even require having any special access to the model or its surrogate – just trying out a small number of *random* rotation and translation combinations already has a significant effect. These findings suggest that our current neural network-based vision models might not be as reliable as we tend to assume.

Finally, we consider a new class of perturbations that combines rotations and translations with the standard pixel-wise attacks. We observe that these two types of input transformations seem to be, in a sense, orthogonal to each other. In particular, the effect of each one of them on the performance of the model seems to be additive, and sometimes even super-additive. Also, robustness to the latter type of perturbations does not seem to have an effect on the robustness to the former type. This suggests that this combined class of transformations is a more complete notion of similarity in the context of adversarial robustness of vision models.

1 Introduction

Neural network models have at this point been widely embraced as cutting-edge solutions in computer vision [18, 13], speech recognition [10], and text analysis [7]. However, despite the near, and sometimes beyond, human-like performance [12, 25] on key benchmarks they offer, it is still not well understood how reliable and robust this performance is. A prominent issue in this context is the existence of so-called *adversarial examples* [24, 9], i.e., inputs that are almost indistinguishable from natural data for a human, yet cause state-of-the-art classifiers to make incorrect predictions

*Equal contribution.

with high confidence. It turns out that not only such inputs exist but they can actually be reliably produced. This raises concerns about the use of neural networks in contexts where reliability, dependability and security matter.

There is now a long line of work on developing methods for training neural network models that are robust to adversarial examples [21, 28, 8, 27, 11]. However, most of these proposed mechanisms were subsequently shown to be vulnerable to more sophisticated attacks [4, 14, 6]. Only recently, it has been demonstrated [20, 3, 16] that robust optimization approaches (also known as adversarial training) can reliably increase the resilience of neural network classifiers to a broad class of adversarial examples. However, a key element required for these approaches to be effective is that the family of adversarial perturbations to be robust to is well-defined.

Therefore, a major challenge that emerges in this context is to precisely define the “right” class of adversarial perturbations we want our models to be resilient to. That is, we need to capture as rigorously as possible what it means for a perturbation of an input to be “imperceptible” or, equivalently, for two inputs to be “similar”. The main notions of similarity studied so far in the context of adversarial examples for image classification are pixel-wise measures based on ℓ_p -norms. Clearly, if two images are close in an ℓ_p -norm, they are usually visually similar as well. The contrapositive, however, does not always hold. There exist simple image transformations that lead to the modified image be far from the original image in all ℓ_p -norms, yet arguably be very similar to it from a human perspective. This raises a fundamental question:

What is a more comprehensive notion of visual similarity for adversarial examples?

In this work, we address this question by studying two fundamental image transformations: translations and rotations. While appearing natural and, in a sense, imperceptible to a human, we show that these transformations *alone*, i.e., without any pixel-wise perturbation added, cause a significant degradation of neural network classification performance. In fact, the robustness to ℓ_∞ -bounded pixel-wise transformations does not even seem to affect the resilience to such rotations and transformations in a significant way. This underlines the need for our current, pixel-wise notions of similarity used in the context of adversarial examples to be significantly broadened. In particular, it should include natural spatial transformations such as rotations and translations.

Additionally, we show that one does not even need to have a direct access to the model (or its surrogate) to find such misclassifying perturbations. In fact, for a significant fraction of inputs, examining even a small number of *random* rotation and translation combinations suffices to find a transformation that leads to misclassification. So, arguably, these kinds of inputs could arise naturally, even in a completely non-adversarial setting. This demonstrates that the existence of adversarial examples and the robustness of our neural network-based models is not only a concern from a safety/security point of view but should also be examined and addressed in the context of “non-adversarial” applications.

1.1 Our Methodology and Results

Our starting point is the MNIST [19] model of Madry et al. [20], which was shown to be robust against a range of adversaries constrained to small perturbations in ℓ_∞ - or ℓ_2 -norm. We demonstrate that small rotations and translations *alone* can cause that model to perform wrong predictions on the entirety of the test set. We extend our experiments to the CIFAR10 [17] and ImageNet [22] datasets, considering both adversarial and random choices of rotations and translation. Even when

the classifiers are not completely fooled, we observe a significant drop in classification accuracy across datasets ranging from 12% to 32% for random perturbations and from 34% to 99% for worst-case perturbations. In fact, choosing the worst out of 10 random transformations is sufficient to reduce the accuracy of these classifiers by 81% on MNIST, 58% on CIFAR10, and 25% on ImageNet (Top 1). These findings demonstrate that CNN classifiers do not automatically generalize to simple image transformations, and that there are significant barriers we need to overcome before they can become truly robust.

We perform extensive experiments that provide a fine-grained understanding of the phenomenon on different datasets. We demonstrate that the inherent properties of each dataset cause the resulting classifiers to have significantly different performance under the simple spatial transformations we consider. In summary, we show that:

- A simple attack based purely on rotations and translations is very effective against neural network classifiers, even when they have been trained to be robust to ℓ_p -bounded adversaries. In fact, ℓ_p -bounded and spatial perturbations seem to be fairly orthogonal to each other and have an additive, and sometimes even super-additive, effect on the classifier’s performance.
- Applying data augmentation using random transformations *does* increase its robustness, but does *not* completely alleviate the issue.
- The fact that the network is fully convolutional does not make it inherently robust to input translations. Achieving such translation invariance requires the training set to contain (or be augmented to contain) a certain amount of translated inputs. Even then, the accuracy under worst-case input translation is significantly worse than the natural, average-case accuracy.

2 Adversarial Rotations and Translations

Recall that, in the context of vision models, an *adversarial example* for a given image x and a classifier C is an image x' that, on one hand, causes the classifier C to output a different label on x' than on x , i.e., to have $C(x) \neq C(x')$, but, on the other hand, is “visually similar” to x . Clearly, the notion of visual similarity is not precisely defined here and, in fact, providing such a precise and rigorous definition is extraordinarily difficult, as it would implicitly require formally capturing the notion of human perception. Consequently, previous work settled on assuming that x and x' are close if and only if $\|x - x'\|_p \leq \varepsilon$ for some $p \in [0, \infty]$ and ε small enough.

This compromise enabled us to make significant progress on understanding the adversarial robustness phenomenon and methods for training robust models. However, it is natural to wonder how much of a compromise we are really making here. Specifically, if a classifier is trained to be robust against perturbations that are constrained in some ℓ_p -norm, is the classifier also robust against other natural transformations of the input images? In this paper, we focus on answering that question in the context of two simple spatial transformations: translations and rotations.

Our point of start is to develop sufficiently strong methods for generating adversarial examples of this type. So far, in the context of pixel-wise perturbations, the most successful approach for constructing adversarial examples has been to use optimization methods on a suitable loss function [24, 9, 5]. Following this approach, we parametrize our attack method with a set of tunable parameters and then optimize over these parameters. We perform this optimization in two distinct ways:

- **First Order Method (FO):** Starting from a random choice of parameters, we iteratively take steps in the direction of the gradient. This is the direction that locally maximizes the loss of the classifier (as a surrogate for misclassification probability). Note that unlike the ℓ_p -norm case, we are not optimizing in the pixel space but in the latent space of rotation and translation parameters.
- **Grid Search:** We first discretize the parameter space and then exhaustively examine every possible parametrization of the attack to find one that causes the classifier to give a wrong prediction (if such a parametrization exists). Since our parameter space is small enough, this method is computationally feasible (in contrast to a grid search for ℓ_p -based adversaries).

We now need to define the exact range of attacks we want to optimize over. For the case of rotation and translation attacks, we wish to find parameters $(\delta u, \delta v, \theta)$ such that rotating the original image θ degrees around the center and then translating it by $(\delta u, \delta v)$ pixels causes the classifier to make a wrong prediction. Formally, the pixel at position (u, v) is moved to the following position (assuming the point $(0, 0)$ is the center of the image):

$$\begin{bmatrix} u' \\ v' \end{bmatrix} = \begin{bmatrix} \cos \theta & -\sin \theta \\ \sin \theta & \cos \theta \end{bmatrix} \cdot \begin{bmatrix} u \\ v \end{bmatrix} + \begin{bmatrix} \delta u \\ \delta v \end{bmatrix}.$$

We implement this transformation in a differentiable manner using the spatial transformer blocks of [15]. In order to deal with pixels mapped to non-integer coordinates, these transformer units include a differentiable bilinear interpolation routine.

Since our loss function is differentiable with respect to the input and the transformation is in turn differentiable with respect to its parameters, we can apply a first-order optimization method to (locally) optimize for the worst-case transformation of the input. By defining the spatial transformation for some x as $T(x; \delta u, \delta v, \theta)$, we construct an adversarial perturbation for x by solving the problem

$$\max_{\delta u, \delta v, \theta} \mathcal{L}(x', y), \quad \text{for } x' = T(x; \delta u, \delta v, \theta), \quad (1)$$

where \mathcal{L} is the loss function of the neural network¹, and y is the correct label for example x . Since this is a non-concave maximization problem, there are no formal guarantees for the global optimality of our solution.

3 Experiments

3.1 Experimental Setup

We will consider standard architectures for the MNIST [19], CIFAR10 [17] and ImageNet [22] datasets. In order to examine to which extent this issue is caused by non-sufficient data augmentation during training, we will examine various data augmentation methods.

Model Architecture For the MNIST dataset we use the convolutional neural network studied by Madry et al. [20]. We removed the extra fully-connected layer so that we have an all-convolutional

¹The loss \mathcal{L} of the classifier is a function from images to real numbers that expresses the performance of the network on the particular example x (e.g., the cross-entropy between predicted and correct distributions).

architecture. This choice does not result in a significantly different behavior (we repeat our experiments for the original models in Appendix C). Both standard and ℓ_∞ -adversarial training code is available online². For CIFAR10, we also consider the naturally and adversarially trained ResNet [13] models³ studied by Madry et al. [20] which obtain at least 45% accuracy against strong adversaries constrained in ℓ_∞ -norm with $\varepsilon = 8$. For efficiency reasons we experiment on the non-wide variant. For ImageNet, we use a ResNet-50 [13] architecture using the code from the `tensorpack` repository [1]. We did not modify the model architectures or training procedures. We will soon make our full experimental code available online.

Attack Space In order to maintain the visual similarity of images to the natural ones we need to restrict the space of allowed perturbations. We consider rotations to be at most 30 degrees and translations to be at most 3 pixels in each direction for MNIST (image size 28×28) and CIFAR10 (image size 32×32), and 24 pixels for ImageNet (image size 299×299). For grid search attacks, we consider 7 values per translation direction and 31 values for rotations, equally spaced. For first-order attacks, we use 200 steps of Projected Gradient Descent of step size 0.01 times the parameter range. When rotating and translating the images, we fill the empty space with zeros (black pixels). We perform additional experiments for mirror padding in Appendix B.

Data Augmentation We consider five variants of training for our models.

- Standard natural training: out-of-the-box training procedure. For CIFAR10 this includes random left-right flipping, random translations of ± 4 , and per image standardization. For ImageNet, it includes random left-right flipping, random cropping similar to that in [23], and various color space transformations. We refer to this as the *Standard* model.
- Standard ℓ_∞ -bounded adversarial training: The classifier is trained using ℓ_∞ -bounded adversarial examples computed using Projected Gradient Descent in the pixel space at each step. For ImageNet there is not yet a classifier that can be efficiently and reliably trained against such an adversary. We refer to this model as *Adversarially Trained*.
- No random cropping: In order to examine the effects of standard data augmentation during training we train the CIFAR10 and ImageNet models without random cropping. We still apply random left-right flips. We refer to this model as *No Crop*.
- Random rotations and translations: We perform a uniformly random perturbation of training examples in the attack space described above at each training step. That is on top of standard data augmentation we translate and rotate the image choosing parameters uniformly at random from the allowed space. We refer to this model as *Augmentation A*.
- Random rotations and translations from larger intervals: Same as Augmentation A, but we instead select random perturbations from a *superset* of the attack space. We sample random rotations of at most 40 degrees and translations of at most 4 pixels for MNIST and CIFAR10, and 32 pixels for ImageNet. We refer to this model as *Augmentation B*.

²https://github.com/MadryLab/mnist_challenge

³https://github.com/MadryLab/cifar10_challenge

3.2 Attack Evaluation

We evaluate all models against random, first order, and grid search (rotations and translations considered both separately and combined) adversaries. The results appear in Table 1 for MNIST, Table 2 for CIFAR10, and Table 3 for ImageNet. We visualize a random subset of successful attacks in Figures 3, 4, 5 of Appendix D respectively.

	Natural	Random	Grid	Trans. Grid	Rot. Grid	FO
Standard	99.06%	83.46%	0.01%	14.20%	66.45%	65.75%
Adversarially Trained	98.43%	81.94%	0.37%	11.54%	65.87%	59.05%
Aug. A ($\pm 3\text{px}$, $\pm 30^\circ$)	99.07%	98.62%	73.36%	92.01%	95.36%	96.68%
Aug. B ($\pm 4\text{px}$, $\pm 40^\circ$)	98.38%	98.47%	84.88%	93.01%	95.73%	96.98%

Table 1: MNIST. Accuracy of different models against rotation and translation adversaries. The allowed transformations are ± 3 pixels translation and $\pm 30^\circ$ rotation (image size is 28×28). The attack parameters are chosen through random sampling, projected gradient descent, or grid search with rotations and translations considered both combined and separate (we also include the original accuracy). The models are the naturally and adversarially trained models of [20]. (first two rows) and the natural model trained using data augmentations with random rotations and translations (± 3 pixels, $\pm 30^\circ$ for augmentation A and ± 4 pixels, $\pm 40^\circ$ for augmentation B).

	Natural	Random	Grid	Trans. Grid	Rot. Grid	FO
Standard	92.62%	60.76%	8.08%	81.31%	24.83%	59.98%
No Crop	90.34%	53.30%	2.01%	57.47%	18.44%	48.66%
Adversarially Trained	80.21%	59.79%	7.20%	59.97%	21.03%	36.64%
Aug. A ($\pm 3\text{px}$, $\pm 30^\circ$)	90.25%	91.09%	59.87%	80.09%	76.33%	85.17%
Aug. B ($\pm 4\text{px}$, $\pm 40^\circ$)	89.55%	91.40%	62.42%	78.56%	76.94%	85.47%

Table 2: CIFAR10. Accuracy of different models against rotation and translation adversaries. The allowed transformations are ± 3 pixels translation and $\pm 30^\circ$ rotation (image size is 32×32). The attack is chosen through random sampling, projected gradient descent, or grid search with rotations and translations considered both combined and separate (we also include the original accuracy). The models are the naturally and adversarially trained models of [20], the standard model trained without random crops, and the standard model trained using data augmentations with random rotations and translations (± 3 pixels, $\pm 30^\circ$ for aug. A and ± 4 pixels, $\pm 40^\circ$ for aug. B).

Despite the high accuracy of standard models on natural examples and their reasonable performance on random perturbations, a grid search adversary can significantly lower the classifiers’ accuracy on the test set. Our first order attack, despite being successful for a considerable number of examples (better than random) is not close to the ground truth. We conjecture that this is due

	Natural	Random	Grid	Trans Grid	Rot Grid	FO
Standard	75.96%	63.39%	31.42%	60.42%	44.98%	63.12%
No Crop	70.81%	59.09%	16.52%	45.17%	34.17%	55.93%
Aug. A (± 24 px, $\pm 30^\circ$)	65.96%	68.60%	32.90%	45.72%	47.25%	66.05%
Aug. B (± 32 px, $\pm 40^\circ$)	66.19%	67.58%	33.86%	44.60%	48.72%	66.14%

Table 3: ImageNet. Top1 accuracy of different models against rotation and translation adversaries. The allowed transformations are ± 24 pixels translation and $\pm 30^\circ$ rotation (image size is 299×299). The attack is chosen through random sampling, projected gradient descent, or grid search with rotations and translations considered both combined and separate (we also include the original accuracy). The models are the standard ResNet-50 from [1], the standard model trained without random crops, and the standard model trained using data augmentations with random rotations and translations (± 24 pixels, $\pm 30^\circ$ for aug. A and ± 32 pixels, $\pm 40^\circ$ for aug. B).

to the problem being so low-dimensional that the non-concavity of the objective is a significant barrier. We visualize the set of fooling angles for a rotations-only grid in Figure 6 of Appendix D and observe that they indeed form a highly non-convex set. This is in contrast to the observations of [20] for pixel-based optimization where PGD is able to reliably find (almost) worst-case examples. We plan to further investigate this issue using more powerful first order adversaries and incorporating random restarts in the procedure.

The addition of random rotations and translations during training greatly improves both the random and adversarial accuracy of the classifier for MNIST and CIFAR10, but less so for ImageNet. Note that the Augmentation B model has been trained on transformations of larger magnitude than those that appear during the evaluation. We don’t observe any significant differences on the *training* accuracy between the standard training and the training utilizing data augmentation (see Table 7 of Appendix D for a comparison).

We perform a fine-grained analysis of the misclassified examples. For each example in each dataset, we examine whether it can be fooled by rotations only, translations only, neither, or both. We visualize the results in Figure 1.

Worst-of- k adversary In order to investigate how brittle these networks are, we analyze the percentage of grid points fooling each classifier. We visualize our findings in Figure 7 in the Appendix D. While the majority of perturbations is benign, there is a significant fraction of them that fools each classifier. This naturally suggests the notion of the following *model-agnostic, non-adaptive* adversary: sample k random perturbations, choose the one with worst model performance. Such an attack is trivial to mount and, according to our results in Table 6 (Appendix D), can significantly degrade the performance of the classifier, even for relatively small values of k . For instance, a worst-of-10 attack reduces the accuracy of the standard classifier from 99% to 18% on MNIST, from 93% to 35% on CIFAR10, and 76% to 51% on ImageNet (Top-1). When training the models with data augmentation, the effectiveness of this attack is reduced, and requires a larger k to achieve close to worst-case classifier performance.

We observe that different datasets exhibit significantly different performance both in a qualitative

and quantitative sense. We outline our observations below.

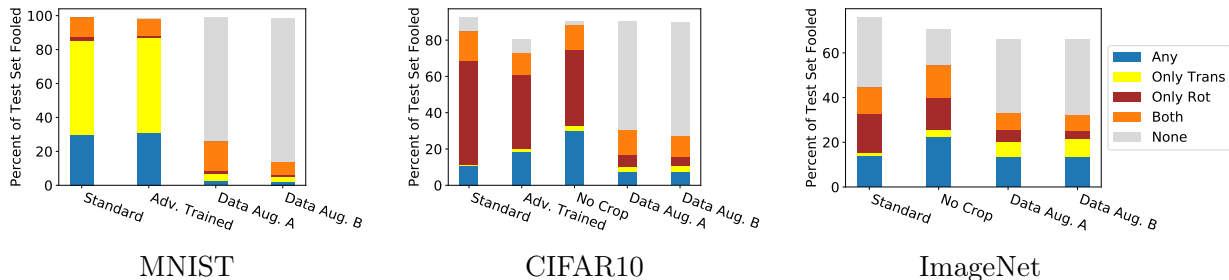


Figure 1: Fine-grained dataset analysis. For each model, we visualize what percent of the test set can be fooled via various methods. We compute how many examples can be fooled with either translations or rotations ("any"), how many can be fooled only by one of these, and how many require a combination to be fooled ("both").

MNIST This is the dataset for which the standard classifier we trained is the most vulnerable to spatial perturbations and can be fooled on the entirety of the test set. Translation only attacks are very effective and can be utilized to fool the model on close to 90% of the test set. Note that in MNIST, digits always appear in the exact center of the image, yet often appear significantly rotated, which partially explains the model’s vulnerability to translation attacks. Since the classifier utilizes convolution and max-pooling units, one might expect it to be more translation-invariant. We find that this is not the case here. We plan to investigate this issue further by examining the network behavior in more detail. Augmenting the dataset with random rotations and translations produces a robust model (>93% accuracy on the test set), and largely alleviates the issue.

CIFAR10 In contrast to MNIST, all the classifiers we trained on CIFAR10 are much more vulnerable to rotations than translation. A rotations-only grid search can fool the standard classifier on more than 70% of its originally correct predictions. Augmenting the dataset with random rotations causes a slight decrease in classification accuracy (around 2%) but increases the accuracy on worst-case rotations and translations to 60% (up from less than 10%).

ImageNet Here, the standard classifier we trained exhibits the most robust behavior. Training on the original dataset with only random left-right flips achieves a Top1 accuracy of 17% (recall that ImageNet contains 1000 classes) against worst-case transformations of the input. The introduction of standard random cropping increases that number to 31% while also increasing natural test-set accuracy from 71% to 76%. Introducing random rotations only yields a 2-3% increase in adversarial robustness, yet reduces natural accuracy by 10%. This behavior indicates that ImageNet has an inherent degree of rotational and translational invariance, which leads to more robust classifiers. The drop in natural accuracy due to data augmentation can possibly be fixed by considering models of larger capacity.

Combining Spatial and ℓ_∞ -bounded perturbations We analyze the performance of an ℓ_∞ -bounded PGD attack for various values of ϵ when combined with random and worst-case spatial

transformation. The experiments are described in Appendix A. We find that, when combined, these attack reduce the classification accuracy in an additive and, in case of MNIST, even super-additive, fashion.

4 Related Work

Recently, [2] and [26] observed independently that it is possible to use various spatial transformations to construct adversarial examples for naturally and adversarially trained models. The main difference to our work is that we show that even very simple transformations (translations and rotations) are already sufficient to break a variety of classifiers, while the transformations employed in [2] and [26] are more involved. The transformation in [2] is based on performing a displacement of individual pixels in the original image that is constrained to be globally smooth and then optimized for misclassification probability. In [26], one considers an ℓ_∞ -bounded pixel-wise perturbation of a version of the original image that has been slightly rotated and a few random pixels have been flipped. Both these methods require direct access to the attacked model (or its surrogate) to compute (or at least estimate) the gradient of the loss function with respect to the model’s input. In contrast, our attacks can be implemented using just a small number of random, non-adaptive transformations of the input.

5 Conclusions

We examined the robustness of state-of-the-art vision classifiers to translations and rotations. We observed that even a small number of randomly chosen perturbations of the input are sufficient to considerably degrade the model performance. Augmenting the training data with such random rotations and translations increases the resulting classifier’s accuracy on such input, but does not completely alleviate the issue. Additionally, we find that classifiers trained to be robust against ℓ_∞ -bounded pixel-based perturbations do not exhibit any additional spatial robustness, suggesting that these are orthogonal concepts.

The vulnerability of state-of-the-art neural networks to such a simple and naturally occurring spatial perturbations indicates that adversarial robustness should be a concern not only in the truly adversarial setting. The finding that such misclassified perturbations can be constructed by trying out a small number of randomly chosen input transformations, emphasizes that such classifiers are indeed quite brittle. Additional techniques need to be incorporated in the architecture and training procedures of modern classifiers to achieve worst-case translational and rotational robustness. Also, these results underline the need for considering broader notions of similarity than just pixel-wise distances when studying adversarial misclassification attacks. In particular, we view combining the pixel-wise distances with rotations and translations as a next step towards capturing the “right” notion of similarity in the context of images.

References

- [1] Tensorpack repository. <https://github.com/ppwyyxx/tensorpack>.
- [2] Anonymous. Spatially transformed adversarial examples. *In submission to International Conference on Learning Representations*, 2018.

- [3] Nicholas Carlini, Guy Katz, Clark Barrett, and David L Dill. Ground-truth adversarial examples. *arXiv preprint arXiv:1709.10207*, 2017.
- [4] Nicholas Carlini and David Wagner. Defensive distillation is not robust to adversarial examples. *arXiv preprint arXiv:1607.04311*, 2016.
- [5] Nicholas Carlini and David Wagner. Towards evaluating the robustness of neural networks. *arXiv preprint arXiv:1608.04644*, 2016.
- [6] Nicholas Carlini and David Wagner. Adversarial examples are not easily detected: Bypassing ten detection methods. *arXiv preprint arXiv:1705.07263*, 2017.
- [7] Ronan Collobert and Jason Weston. A unified architecture for natural language processing: Deep neural networks with multitask learning. In *Proceedings of the 25th international conference on Machine learning*, pages 160–167. ACM, 2008.
- [8] Reuben Feinman, Ryan R Curtin, Saurabh Shintre, and Andrew B Gardner. Detecting adversarial samples from artifacts. *arXiv preprint arXiv:1703.00410*, 2017.
- [9] Ian J. Goodfellow, Jonathon Shlens, and Christian Szegedy. Explaining and harnessing adversarial examples. *arXiv preprint arXiv:1412.6572*, 2014.
- [10] Alex Graves, Abdel-rahman Mohamed, and Geoffrey Hinton. Speech recognition with deep recurrent neural networks. In *Acoustics, speech and signal processing (icassp), 2013 ieee international conference on*, pages 6645–6649. IEEE, 2013.
- [11] Kathrin Grosse, Praveen Manoharan, Nicolas Papernot, Michael Backes, and Patrick McDaniel. On the (statistical) detection of adversarial examples. *arXiv preprint arXiv:1702.06280*, 2017.
- [12] Kaiming He, Xiangyu Zhang, Shaoqing Ren, and Jian Sun. Delving deep into rectifiers: Surpassing human-level performance on imagenet classification. In *Proceedings of the IEEE international conference on computer vision*, pages 1026–1034, 2015.
- [13] Kaiming He, Xiangyu Zhang, Shaoqing Ren, and Jian Sun. Deep residual learning for image recognition. In *Proceedings of the IEEE Conference on Computer Vision and Pattern Recognition*, pages 770–778, 2016.
- [14] Warren He, James Wei, Xinyun Chen, Nicholas Carlini, and Dawn Song. Adversarial example defenses: Ensembles of weak defenses are not strong. *arXiv preprint arXiv:1706.04701*, 2017.
- [15] Max Jaderberg, Karen Simonyan, Andrew Zisserman, et al. Spatial transformer networks. In *Advances in Neural Information Processing Systems*, pages 2017–2025, 2015.
- [16] J Zico Kolter and Eric Wong. Provable defenses against adversarial examples via the convex outer adversarial polytope. *arXiv preprint arXiv:1711.00851*, 2017.
- [17] Alex Krizhevsky and Geoffrey Hinton. Learning multiple layers of features from tiny images. 2009.
- [18] Alex Krizhevsky, Ilya Sutskever, and Geoffrey E Hinton. Imagenet classification with deep convolutional neural networks. In *Advances in neural information processing systems*, pages 1097–1105, 2012.

- [19] Yann LeCun, Léon Bottou, Yoshua Bengio, and Patrick Haffner. Gradient-based learning applied to document recognition. *Proceedings of the IEEE*, 86(11):2278–2324, 1998.
- [20] Aleksander Madry, Aleksandar Makelov, Ludwig Schmidt, Dimitris Tsipras, and Adrian Vladu. Towards deep learning models resistant to adversarial attacks. *arXiv preprint arXiv:1706.06083*, 2017.
- [21] Nicolas Papernot, Patrick McDaniel, Xi Wu, Somesh Jha, and Ananthram Swami. Distillation as a defense to adversarial perturbations against deep neural networks. In *Security and Privacy (SP), 2016 IEEE Symposium on*, pages 582–597, 2016.
- [22] Olga Russakovsky, Jia Deng, Hao Su, Jonathan Krause, Sanjeev Satheesh, Sean Ma, Zhiheng Huang, Andrej Karpathy, Aditya Khosla, Michael Bernstein, Alexander C. Berg, and Li Fei-Fei. ImageNet Large Scale Visual Recognition Challenge. *International Journal of Computer Vision (IJCV)*, 115(3):211–252, 2015.
- [23] Christian Szegedy, Wei Liu, Yangqing Jia, Pierre Sermanet, Scott Reed, Dragomir Anguelov, Dumitru Erhan, Vincent Vanhoucke, and Andrew Rabinovich. Going deeper with convolutions. In *Proceedings of the IEEE conference on computer vision and pattern recognition*, pages 1–9, 2015.
- [24] Christian Szegedy, Wojciech Zaremba, Ilya Sutskever, Joan Bruna, Dumitru Erhan, Ian J. Goodfellow, and Rob Fergus. Intriguing properties of neural networks. *arXiv preprint arXiv:1312.6199*, 2013.
- [25] Yaniv Taigman, Ming Yang, Marc’Aurelio Ranzato, and Lior Wolf. Deepface: Closing the gap to human-level performance in face verification. In *Proceedings of the IEEE conference on computer vision and pattern recognition*, pages 1701–1708, 2014.
- [26] Florian Tramèr and Dan Boneh. Personal communication, 2017.
- [27] Florian Tramèr, Alexey Kurakin, Nicolas Papernot, Dan Boneh, and Patrick D. McDaniel. Ensemble adversarial training: Attacks and defenses. *arXiv preprint arXiv:1705.07204*, 2017.
- [28] Weilin Xu, David Evans, and Yanjun Qi. Feature squeezing: Detecting adversarial examples in deep neural networks. *arXiv preprint arXiv:1704.01155*, 2017.

A Combining Spatial and ℓ_∞ -bounded Adversaries

We also consider the performance of an adversary that utilizes simple spatial transformations combined with small ℓ_∞ -bounded perturbations. For different values of ε we compute the performance of a PGD adversary constrained to be within ε in ℓ_∞ -norm from the original or spatially perturbed image. When combining with a spatial grid-search adversary we perform an independent PGD attack on each point of the grid and choose the worst one. The results are shown in Figure 2.

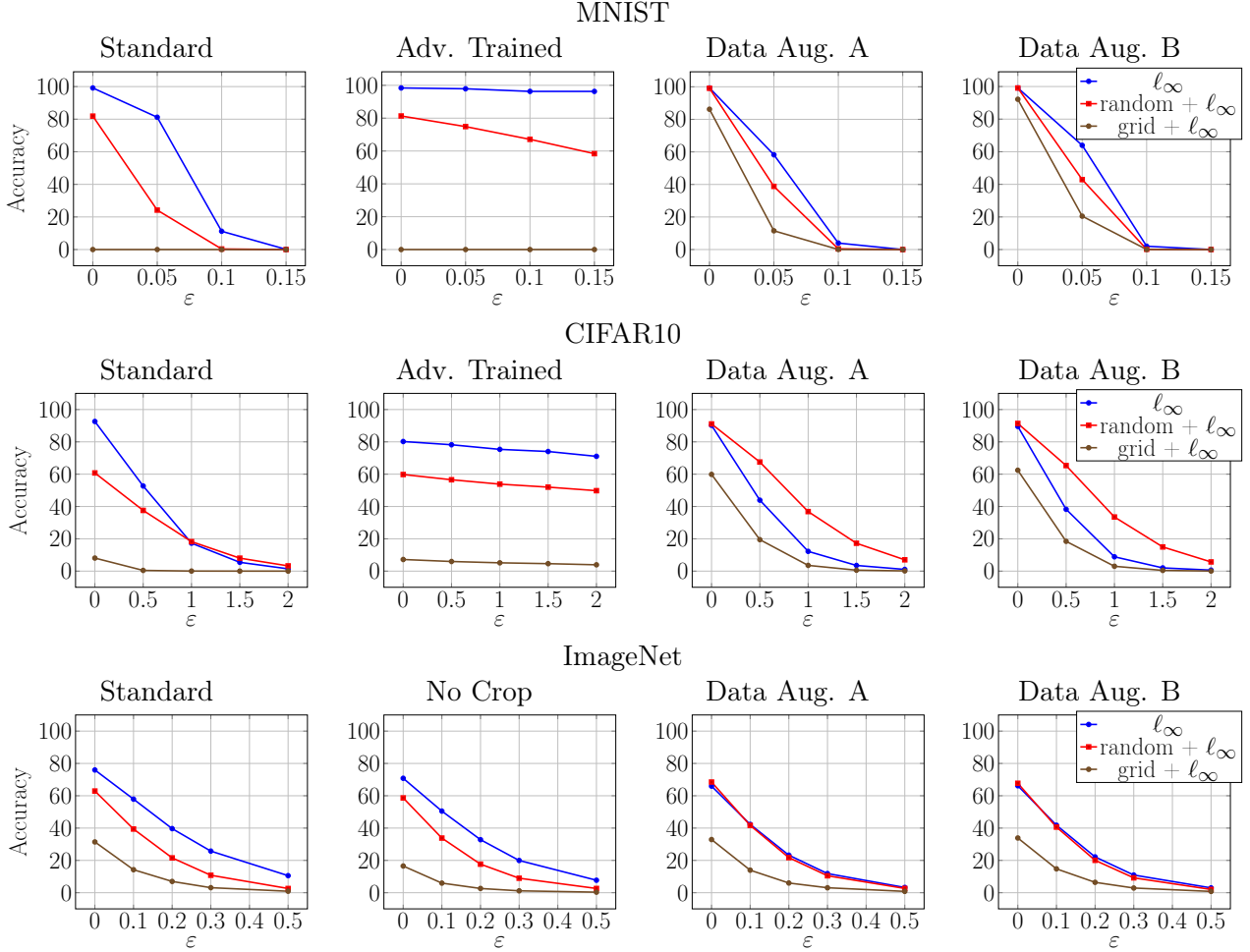


Figure 2: Accuracy of different classifiers against ℓ_∞ -bounded adversaries with various values of ε and spatial transformations. For each value of ε , we perform PGD to find the most adversarial ℓ_∞ -bounded perturbation. Additionally, we combine PGD with random rotations and translations and with a grid search over rotations and translations in order to find the transformation that combines with PGD in the most adversarial way.

We observe that spatial and ℓ_∞ -bounded perturbations have an additive effect on the classification accuracy. For MNIST, this effect is super-additive, possibly due to the bilinear interpolation. On the data-augmented CIFAR10 models, we observe that random spatial perturbations of the

input are harder for the PGD adversary to attack. We don't have an explanation for this behavior.

B Mirror Padding

In the experiments of Section 3, we filled the remaining pixels of rotated and translated images with black (also known as zero or constant padding). This is the standard approach used when performing random cropping for data augmentation purposes. We briefly examined the effect of mirror padding, that is replacing empty pixels by reflecting the image around the border⁴. The results are shown in Table 4. We observed that training with one padding method and evaluating using the other resulted in a significant drop in accuracy. Training using one of these methods randomly for each example resulted in a model which roughly matched the best-case of the two individual cases.

	Natural	Random (Zero)	Random (Mirror)	Grid Search (Zero)	Grid Search (Mirror)
Standard Nat	92.62%	60.76%	66.42%	8.08%	5.37%
Standard Adv	80.21%	59.79%	67.12%	7.20%	12.89%
Aug. A, Zero	90.25%	91.09%	87.67%	59.87%	40.55%
Aug. B, Zero	89.55%	91.40%	87.94%	62.42%	42.37%
Aug. A, Mirror	92.25%	88.43%	91.05%	41.46%	53.95%
Aug. B, Mirror	92.03%	88.58%	91.34%	45.44%	57.97%
Aug. A, Both	91.80%	90.98%	91.28%	56.95%	52.60%
Aug. B, Both	91.57%	91.87%	91.11%	60.46%	56.13%

Table 4: CIFAR10: The effect of using reflection or zero padding when training a model. The experimental setup matches that of Section 3. Zero padding refers to filling the empty pixels caused by translations and rotations with black. Mirror padding corresponds to using a reflection of the images. "Both" refers to training using both methods and alternating randomly between them for each training example.

C Original Madry et al. Models

In addition to the fully convolutional networks considered in Section 3, we consider the original models of [20] available online⁵ as well as the corresponding data augmented variant we train ourselves. The results are shown in Table 5. We don't observe any qualitative difference between the two variants.

⁴https://www.tensorflow.org/api_docs/python/tf/pad

⁵https://github.com/MadryLab/mnist_challenge

	Natural	Random	Grid	Trans. Grid	Rot. Grid	FO
Standard	99.17%	81.88%	0.01%	11.86%	68.20%	63.78%
Adversarially Trained	98.40%	81.33%	0.00%	8.24%	66.83%	73.61%
Aug. A ($\pm 3\text{px}$, $\pm 30^\circ$)	99.37%	99.19%	88.17%	96.23%	97.73%	98.55%
Aug B ($\pm 4\pm$, $\pm 40^\circ$)	99.22%	99.24%	93.50%	96.96%	98.00%	98.67%

Table 5: MNIST. Accuracy of the original models of [20] and their data augmented variants. The only difference of this architecture from the one considered in the main paper body is the introduction of a fully-connected layer of size 1024 before the softmax layer. The evaluation experiments are exactly the same as those in Table 1.

D Omitted Tables and Figures

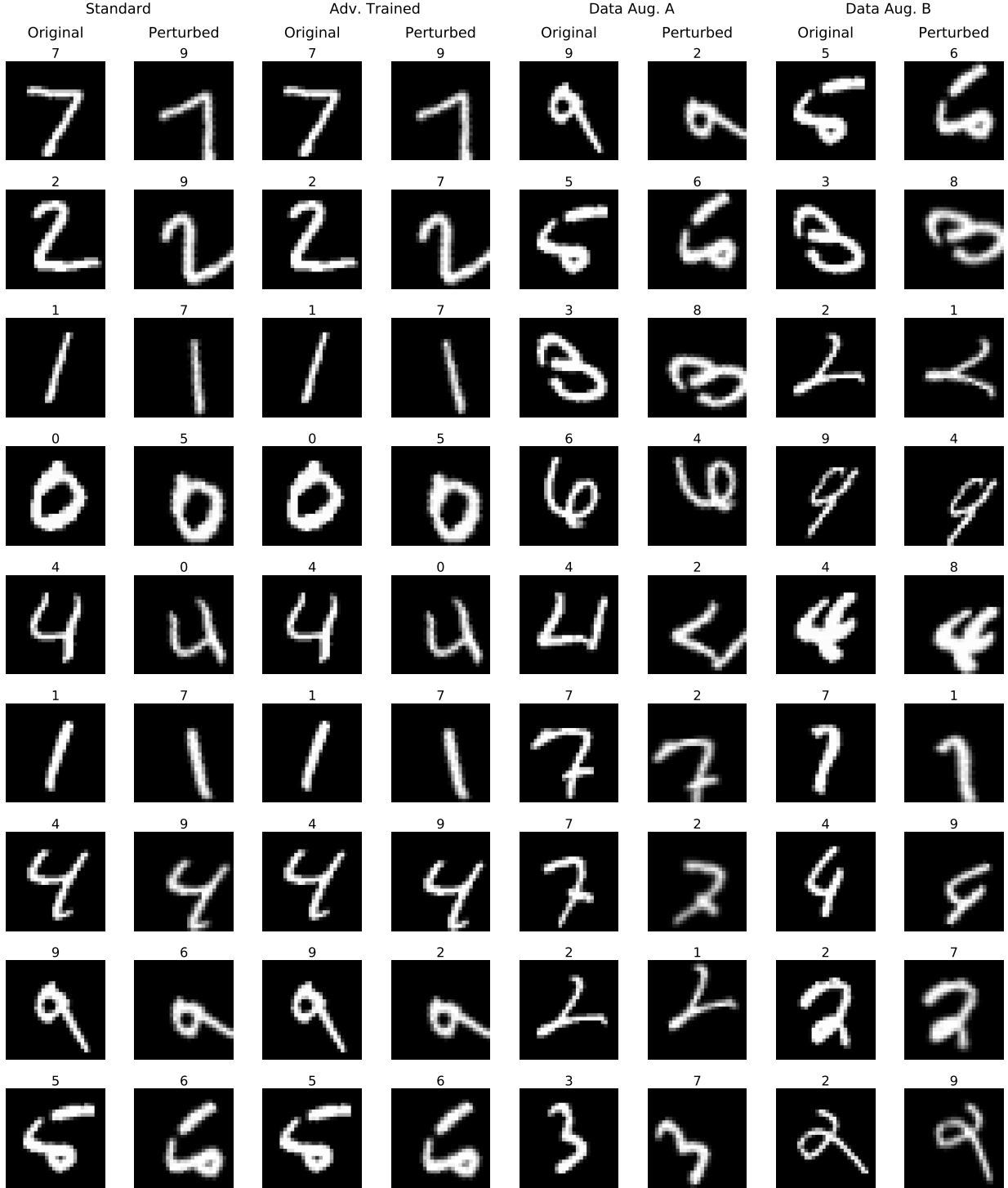


Figure 3: MNIST. Successful adversarial examples for the models studied in Section 3. Rotations are restricted to be within 30° of the original and translations up to 3 pixels per directions (image size 28×28). Each example is visualized along with its predicted label in the original and perturbed version.

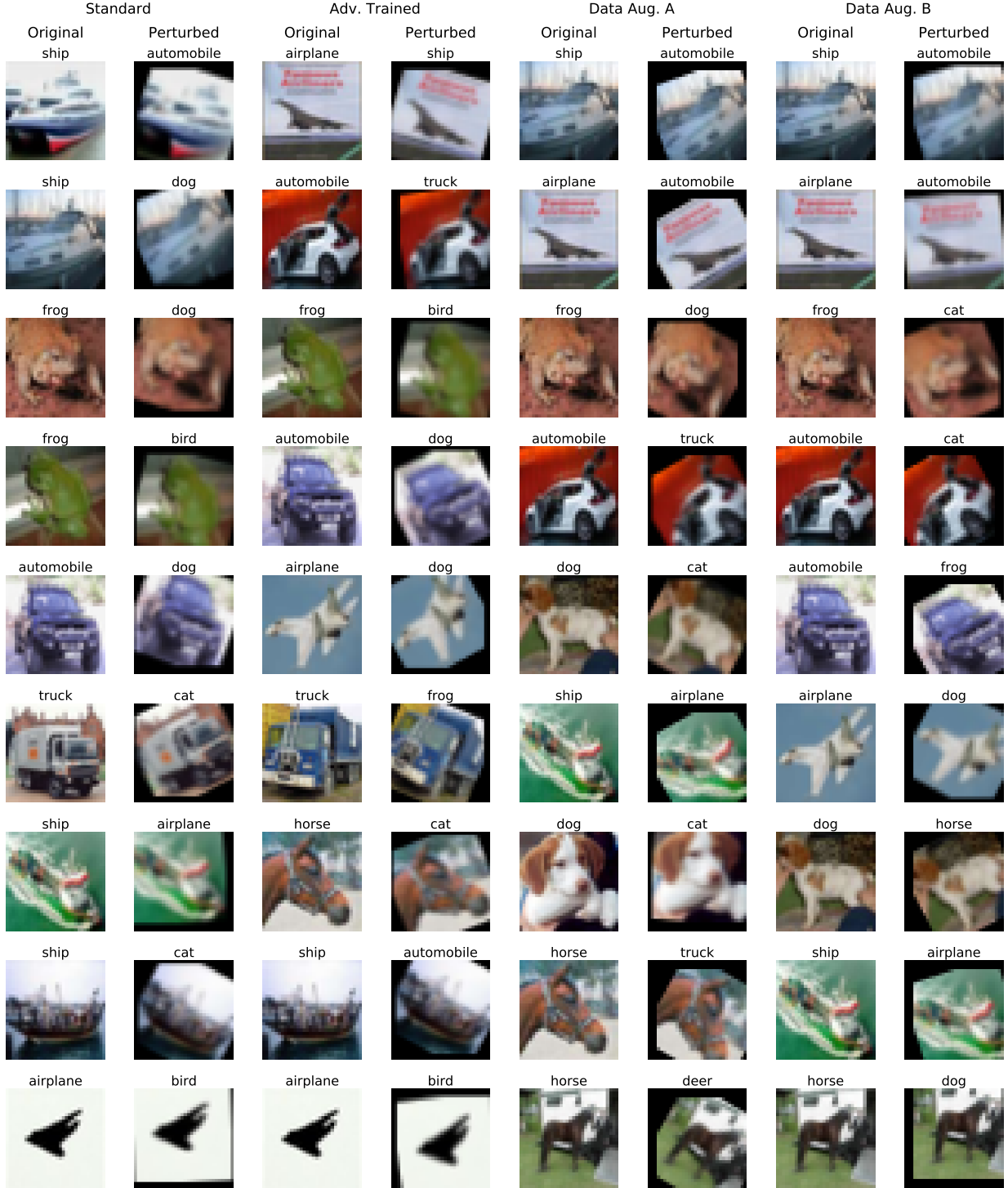


Figure 4: CIFAR10. Successful adversarial examples for the models studied in Section 3. Rotations are restricted to be within 30° of the original and translations up to 3 pixels per directions (image size 32×32). Each example is visualized along with its predicted label in the original and perturbed version.

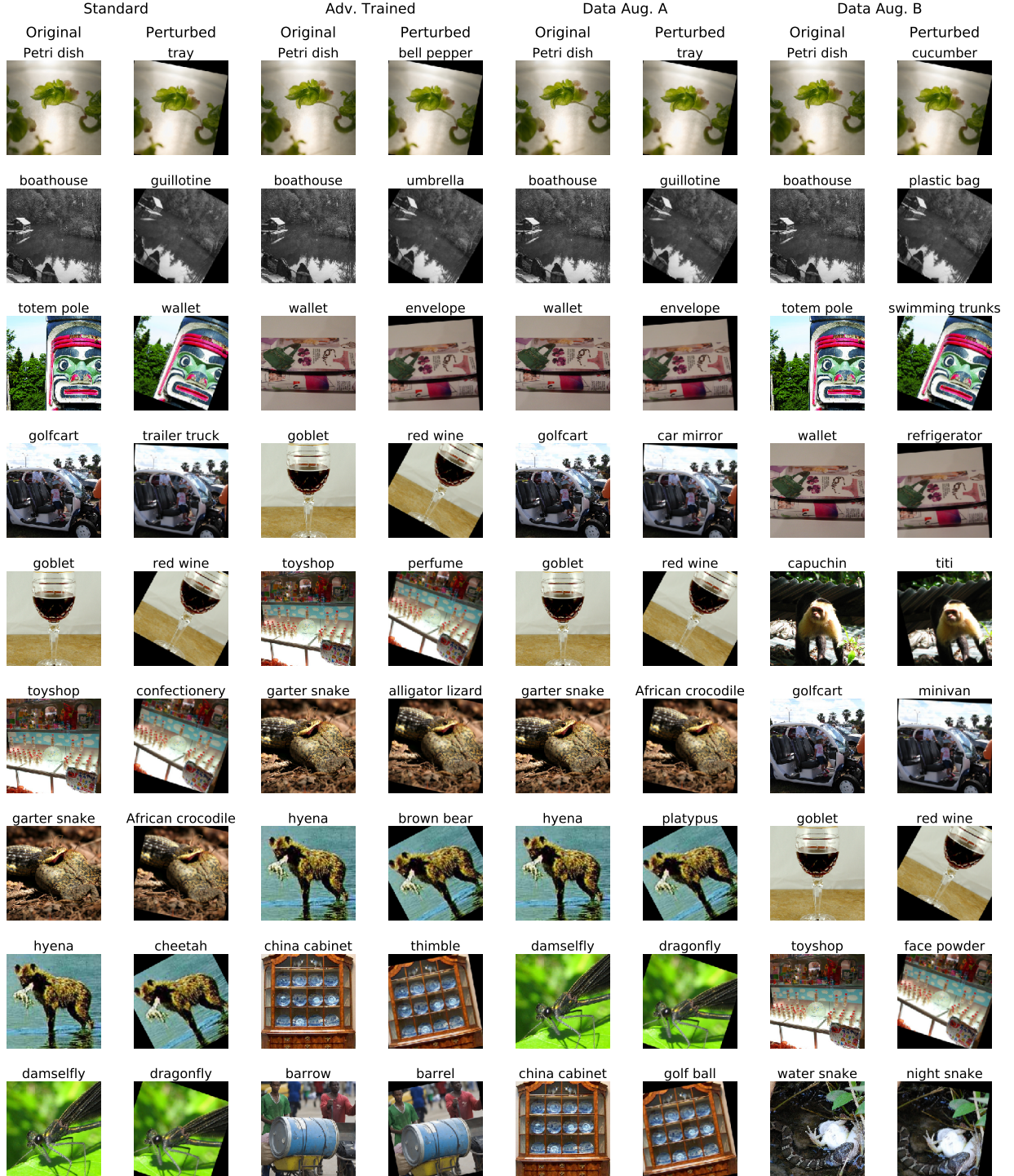


Figure 5: ImageNet. Successful adversarial examples for the models studied in Section 3. Rotations are restricted to be within 30° of the original and translations up to 24 pixels per directions (image size 299×299). Each example is visualized along with its predicted label in the original and perturbed version.

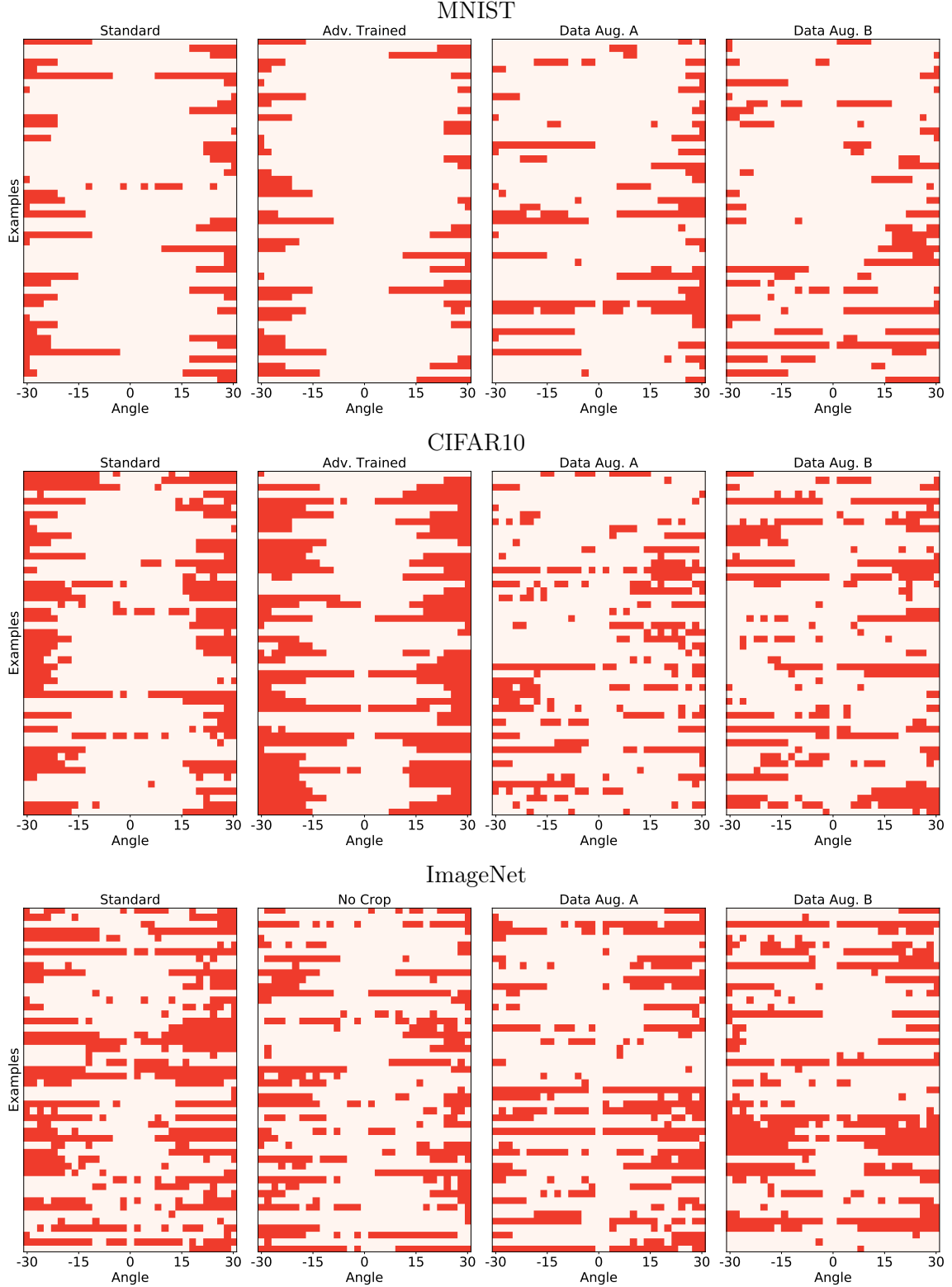


Figure 6: Visualizing which angles fool the classifier for 50 random examples. For each dataset and model, we visualize one example per row. Red corresponds to *misclassification* of the images. We observe that the angles fooling the models form a highly non-convex set.

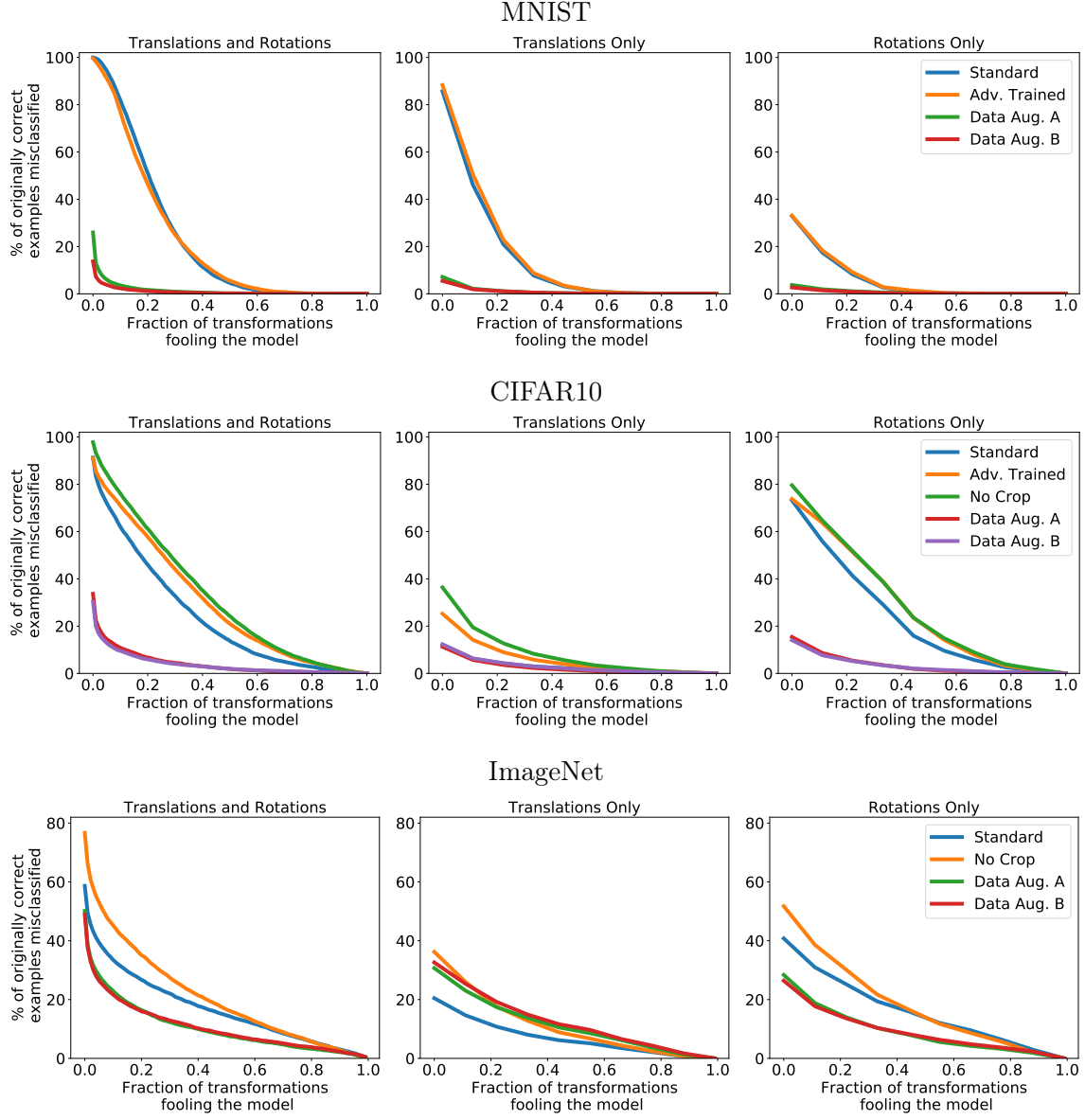


Figure 7: Cumulative Density Function plots. For each percentage of grid points p , we plot the percentage of correctly classified test set examples that are fooled by at least $p\%$ of the grid points.

MNIST					
	Standard	Adv. Trained	Aug. A	Aug. B.	
Natural	99.06%	98.43%	99.07%	98.38%	
Random	83.46%	81.94%	98.62%	98.47%	
Worst-of-10	18.23%	23.03%	95.55%	96.12%	
Worst-of-100	0.36%	1.71%	86.02%	91.17%	
Worst-of-1000	0.02%	0.46%	76.08%	86.11%	
Worst-of-1519	0.01%	0.37%	73.36%	84.88%	

CIFAR					
	Standard	No Crop	Adv. Trained	Aug. A	Aug. B.
Natural	92.62%	90.34%	80.21%	90.25%	89.55%
Random	60.76%	53.30%	59.79%	91.09%	91.40%
Worst-of-10	35.36%	21.74%	23.43%	80.50%	81.01%
Worst-of-100	15.26%	6.00%	11.43%	69.82%	71.66%
Worst-of-1000	9.25%	2.52%	7.88%	62.11%	64.69%
Worst-of-1519	8.08%	2.01%	7.20%	59.87%	62.42%

ImageNet					
	Standard	No Crop	Aug. A	Aug. B.	
Natural	75.96%	70.81%	65.96%	66.19%	
Random	63.39%	59.09%	68.60%	67.58%	
Worst-of-10	50.52%	38.80%	50.85%	51.86%	
Worst-of-100	38.34%	23.95%	40.47%	41.22%	
Worst-of-1000	31.42%	16.52%	32.90%	33.86%	
Worst-of-1519	31.42%	16.52%	32.90%	33.86%	

Table 6: We consider the performance of an adversary that samples k perturbations uniformly at random and uses the worst one for the classifier (“Worst-of- k ” adversary). That is, for each k we compute what percentage of the test set can be fooled by at least a $1/k$ fraction of the grid of all possible perturbations. Since the grid we consider has size $7 \times 7 \times 31$, “worst-of-1519” is the strongest adversary, equivalent to a grid search. We observe that even 10 random samples are sufficient to fool a significant fraction of the test set.

	MNIST	CIFAR10	ImageNet
Standard	100.00%	100.00%	77.71%
No Crop	-	100.00%	97.97%
Aug. A	98.09%	99.25%	74.72%
Aug. B	97.68%	98.18%	76.16%
Adv. Trained	85.42%	57.13%	-

Table 7: Training accuracy of each model. This is computed on the perturbed version of the dataset (including rotations, translations or ℓ_∞ -bounded perturbations). We do not observe significant differences between standard training and rotation/translation augmented training.